Journal of Biomechanics 108 (2020) 109880

Contents lists available at ScienceDirect

Journal of Biomechanics

journal homepage: www.elsevier.com/locate/jbiomech
www.JBiomech.com

Maxillary suture expansion: A mouse model to explore the molecular effects of mechanically-induced bone remodeling

Jose Alejandro Guerrero [a,1], Raquel Souto Silva [b,1], Izabella Lucas de Abreu Lima [c], Bianca Cristina Duffles Rodrigues [c], Breno Rocha Barrioni [d], Flávio Almeida Amaral [e], André Petenuci Tabanez [f], Gustavo Pompermaier Garlet [g], Diego Alexander Garzon Alvarado [h], Tarcília Aparecida Silva [i], Estevam Barbosa de Las Casas [j], Soraia Macari [k,*]

[a] Institute of Biotechnology, Department of Mechanical and Mechatronic Engineering, Faculty of Engineering, National University of Colombia, Bogotá, Colombia
[b] Departament of Social and Preventive Dentistry, Faculty of Dentistry, Federal University of Minas Gerais, Belo Horizonte, MG, Brazil
[c] Departament of Pediatric Dentistry, Faculty of Dentistry, Federal University of Minas Gerais, Belo Horizonte, MG, Brazil
[d] Department of Metallurgical and Materials Engineering, Faculty of Engineering, Federal University of Minas Gerais, Belo Horizonte, MG, Brazil
[e] Department of Biochemistry and Immunology, Institute of Biological Sciences, Federal University of Minas Gerais, Belo Horizonte, MG, Brazil
[f] Department of Biological Sciences, Faculty of Dentistry of Bauru, University of São Paulo, Bauru, SP, Brazil
[g] Department of Biological Sciences, Faculty of Dentistry of Bauru, University of São Paulo, Bauru, SP, Brazil
[h] Institute of Biotechnology, Department of Mechanical and Mechatronic Engineering, Faculty of Engineering, National University of Colombia, Bogotá, Colombia
[i] Department of Clinic, Pathology and Dental Surgery, Faculty of Dentistry, Federal University of Minas Gerais, Belo Horizonte, MG, Brazil
[j] Department of Structural Engineering, Faculty of Engineering, Federal University of Minas Gerais, Belo Horizonte, MG, Brazil
[k] Department of Restorative Dentistry, Faculty of Dentistry, Federal University of Minas Gerais, Belo Horizonte, MG, Brazil

ARTICLE INFO

Article history:
Accepted 9 June 2020

Keywords:
Maxillary suture expansion
Orthodontics
Bone remodeling
Experimental model
Biomarkers
Molecular analysis

ABSTRACT

The aim of this study was to analyze the effect of rapid maxillary expansion (RME) on hard tissues. Opening loops bonded to the first and second maxillary molars on both sides were used to apply distracting forces of 0.28 N, 0.42 N and 0.56 N at the midpalatal suture for 7 and 14 days. Microcomputed tomography (MicroCT), histomorphometry and quantitative polymerase chain reaction (qPCR) analysis were performed to evaluate RME effectiveness, midpalatal suture remodeling, cell counting of osteoblasts, osteoclasts and chondrocytes and the expression of bone remodeling markers, respectively. All forces at the two different time points resulted in similar RME and enhanced of bone remodeling. Accordingly, increased number of osteoblasts and reduced chondrocytes counting and no difference in osteoclasts were seen after all RME protocols. RME yielded increased expression of bone remodeling markers as osteocalcin (Ocn), dentin matrix acidic phosphoprotein-1 (Dmp1), runt-related transcription factor 2 (Runx2), collagen type I Alpha 1 (Col1a1), alkaline phosphatase (ALP), receptor activator of nuclear factor kappa B (RANK), receptor activator of nuclear factor kappa B ligand (Rankl), osteoprotegerin (Opg), cathepsin K (Ctsk), matrix metalloproteinases 9 and 13 (Mmp9 and 13), transforming growth fator beta 1, 2 and 3 (Tgfb 1, Tgfb 2 and Tgfb3), bone morphogenetic protein 2 (Bmp-2), sclerostin (Sost), beta-catenin-like protein 1 (Ctnnbl) and Wnt signaling pathways 3, 3a and 5a (Wnt 3, Wnt 3a and Wnt 5a). These findings characterize the cellular changes and potential molecular pathways involved in RME, proving the reliability of this protocol as a model for mechanical-induced bone remodeling.

1. Introduction

Rapid maxillary expansion (RME) results in widening of maxilla by separation of the midpalatal suture and the circummaxillary sutural system (McNamara, 2006). The maxillary suture is situated between the maxillary bones in the palate and it is extremely responsive to mechanical loads (Cheng et al., 2018; Copray et al., 1985; Hinton, 1988; Kantomaa et al., 1994). RME is routinely used

* Corresponding author at: Departamento de Odontologia Restauradora, Faculdade de Odontologia, Universidade Federal de Minas Gerais, Av. Presidente Antônio Carlos 6627, CEP 31.270-901, Belo Horizonte, Minas Gerais, Brazil.
E-mail address: soraiamacari@gmail.com (S. Macari).
[1] Authors contributed equally.

https://doi.org/10.1016/j.jbiomech.2020.109880
0021-9290/

to correct maxillary width deficiencies and malocclusions (Bishara and Staley, 1987) and to assist correction of Angle Class II (Guest et al., 2010) and Class III malocclusions (da Silva Filho et al., 1998).

RME success depends on bone remodeling (Jiao et al., 2015; Raisz, 1999; Schett and Teitelbaum, 2009) which relies on bone resorption and deposition (Riancho and Delgado-Calle, 2011; Tanaka et al., 2005). These processes ensure the homeostasis, growth and restoration of any bone damage and allow the adaptation to mechanical conditions (Raggatt and Partridge, 2010). Mechanical loading is a potent inducer of bone remodeling (Hadjidakis and Androulakis, 2006) and different models are available as orthodontic tooth movement (Lima et al., 2017; Macari et al., 2018b; Taddei et al., 2012) and RME (Byron et al., 2004; Henderson et al., 2005; Hou et al., 2007, 2009; Vij and Mao, 2006; Wu et al., 2017). These models are useful not only in orthodontics, but also have a potential to be used in studies seeking pharmacological targets for bone diseases.

In order to achieve efficient protocols for bone remodeling and provide biomechanical models for cellular and morphological studies, craniofacial sutures in rats (Byron et al., 2004; Henderson et al., 2005; Vij and Mao, 2006; Wu et al., 2017) and mice (Hou et al., 2007, 2009) were exposed to mechanical loading. However, there is no standardization of applied forces that induces RME in the maxilla suture and demonstration of molecular changes during bone remodeling at different time points. Definition of time and force is pivotal to minimize deleterious effects on soft and hard tissues (Krishnan and Davidovitch, 2006; Ren et al., 2007). Therefore, we aimed to develop a standardized RME protocol to analyze the kinetics of molecular markers and bone cells recruitment to midpalatal suture subjected to mechanical force in mice.

2. Materials and methods

2.1. Animals

Five-week-old wild-type (WT) (C57BL6/J) mice were obtained from Animal Care Facilities and were treated under Institutional Ethics Committee (#152/2016). Six mice were used for controls (without coil) and experimental (with activated coil) groups at each timepoint; and 4 mice were used as sham operated (with inactivated coil). Each animal weight was recorded throughout the experimental period. Mice were maintained under a standard condition with a 12 h light/dark cycle, controlled temperature (24 ± 2 °C) and free access to commercial chow and drinking water. After appliance installation, mice were fed with pasty chow.

2.2. RME protocol

Mice were anesthetized using a combination of xylazine (10 mg/Kg) and ketamine (100 mg/Kg) and placed in a dorsal decubitus position, with the 4 limbs affixed to a surgical table (Fig. 1A). To permit the full visualization of intra-oral structures, a mouth-opener (Fig. 1B) was affixed to the surgical table with a 0.08 mm wire to inhibit any movement of the head.

A stereomicroscope (Quimis Aparelhos Científicos Ltd, Diadema, São Paulo, Brazil) and an optical light system (Multi-Position Fiber Optic Illuminator system, Cole-Parmer Instrument Company Ltd., London, England) were used to better visualize the intra-oral structures. The left and right first and second maxillary molars surfaces were etched using a self- etching primer (Unitek/3 M, Minneapolis, USA). To apply a distracting force to the midpalatal suture, opening loops were made using 0.014-inch stainless steel orthodontic wire (GAC International Inc., Bohemia, NY) and bonded to the occlusal surface of maxillary molars on both sides using a light-cured resin (Transbond, Unitek/3 M, Monrova, CA, USA) (Fig. 1E-F). To minimize errors through the procedures the same operator was responsible to manufacturer the coils and its attachment in all mice.

To guarantee the force value of the opening loop, force magnitude was calibrated by a tension gauge (Shimpo Instruments, Itasca, Ill) to exert 0.28 N, 0.42 N or 0.56 N (Fig. 1C-D). The loops were not reactivated throughout the experimental period. Animals with no opening loop were used as control. Not activated loops were used in sham operated mice. After 7 and 14 days, animals were euthanized by decapitation and the suture analyzed by micro-computed tomography (microCT) and histology. The analyses were conducted by one observer and for the intra observer calibration, except for qPCR analysis; at least three measurements

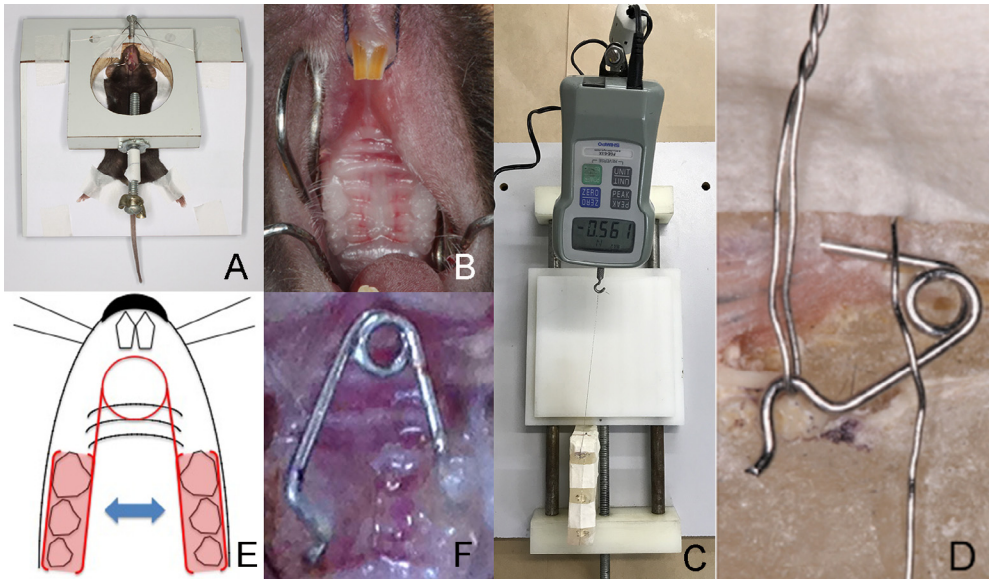

Fig. 1. Experimental protocol. (A) Mice positioned in the dorsal decubitus on the surgical table to restrict animal movement and to permit intra-oral access. (B) Mouth-opener in position and the occlusal view of the maxillary molar region. (C) A tension gauge attached to the table that stabilizes the opening loops showing 0.56 N of mechanical loading. (D) A positioned opening loop activation (E) Scheme showing the bonded loop and force direction. (F) Opening loops bonded to the occlusal surface of the upper molars.

were performed for each parameter. The data were compared using Kappa statistic. The observer was calibrated until the measurements of each analysis reached a Kappa value above 0.81.

2.3. MicroCT imaging

After euthanasia, maxillae were dissected and fixed in 10% buffered formalin (pH 7.4). With the opening coil appliance in situ, maxillae were scanned using a compact desktop microCT scanner Skyscan 1174 (Bruker-MicroCT, Belgium) according to Macari et al. (Macari et al., 2018a).

The palatal/maxillary bones width (μm) were measured in the transaxial position as the mean distance between: (1) the occlusal third and middle third obtained at the root canal of the incisors; (2) the occlusal third and middle third obtained at the vestibular surface of the mesio-vestibular root of the first molar; and, (3) middle third and apical third obtained at the palatal root canal of the first molar. The 3D volume (μm^3) of the RME was performed by selecting coronal antero-posterior palatal bone regions to obtain the region of interest at the first molar level.

The effects of RME in the microarchitecture of palatal bones were analyzed. Regular and uniformly oblong shaped region of interest was used as contouring method to delineate the region of interest (ROI) in midpalatal area. The tissue was analyzed (CTan, Bruker-MicroCT, Belgium) to determine bone mineral density (BMD g/cm^{-3}), percent bone volume/tissue volume (BV/TV %), bone volume (BV μm^3), trabecular number (Tb.N mm^{-1}), trabecular separation (Tb.Sp) and trabecular thickness (Tb.Th μm) (Bouxsein et al., 2010). An investigation with different thresholds values was performed to establish robust parameters (Supplemental Material and Supplemental Fig. 1A-C).

2.4. Histological analysis of midpalatal suture

The same maxillae submitted to microCT were decalcified in 14% EDTA (pH 7.4) for 21 days and routine histological processing was performed. Maxillae included in paraffin were cut in the coronal into 4 μm thickness sections.

Masson's trichrome staining was used for osteoblasts analysis in the midpalatal suture. The cell counting was determined in the marginal bone contouring the maxillary suture at the level of the palatal root of the first molar. At least five serial vertical sections containing the above mentioned structures were evaluated for each animal.

Tartrate resistant acid phosphatase (TRAP; Sigma-Aldrich, Saint Louis, MO, USA), stained sections were used for counting osteoclasts at the marginal bone contouring the maxillary suture at the level of the palatal root of the first molar.

2.5. Histopathological analysis of nasal cartilage

Histopathological changes of nasal cartilage were evaluated by one pathologist (T.A.S) in H&E and Masson's trichrome stained sections. Changes analyzed in five consecutive microscopic fields and marked as positive/negative and scored in 0 (no changes), 1 or 2 when less than 50% or more than 50% of cartilage area was involved, respectively. Results were expressed as % of positive cases for each score. The chondrocytes in the nasal area were counted using the Image J software (National Institutes of Health, USA). Results were expressed as number of chondrocytes per mm^2.

2.6. Quantitative polymerase chain reaction (qPCR)

Total RNA was extracted from tissues of the midpalatal region (RNeasy FFPE kit; Qiagen Inc., Valencia, CA), according to the manufacturer's instructions. The complementary cDNA synthesis and Real-Time PCR array were performed according to Macari et al. (2018a). The targets analyzed and basic reactions are shown in Supplemental Table 1. The mean Ct values from duplicate measurements were used to calculate expression of the target gene, with normalization to an internal control (β-actin) using the $2^{-\Delta\Delta Ct}$ method.

2.7. Statistical analysis

Results were expressed as mean ± standard deviation (SD). Two-way ANOVA followed by the Bonferroni *post-hoc* test was used to analyze differences among groups (GraphPad 5.01 Software, San Diego, CA). $P < 0.05$ was considered statistically significant.

3. Results

3.1. Defining the optimal force and timing for RME

Sham operated (with inactivated coil) and control (no coil) groups exhibited similar quantification of midpalatal suture distraction and area gained in the midpalatal suture after RME (Figs. 2A-C and 3A-B). Also, considering the measurement at middle third and apical third obtained at the palatal root canal of the first molar similar RME was observed comparing 7 and 14 days (3208 μm ± 57.2 μm; 3099 μm ± 52.44 μm, respectively) and three tensile forces of 0.28 N (7d: 4949 μm ± 70.86 μm; 14d: 4905 μm ± 55.87 μm), 0.42 N (7d: 4937 μm ± 129.9 μm; 14d: 4977 μm ± 127.7 μm) and 0.56 N (7d: 4783 μm ± 45.36 μm; 14d: 5067 μm ± 121.1 μm) (Fig. 2A-B). Taking into account the mean of both controls (7 and 14 days) and the mean of all experimental groups there was an increase of 56.6% of the distance of the palatal bones in the midpalatal suture after RME. Significant changes were seen when comparing measurements taken from all dental references that considered the first molars. However when the middle third and apical third of the palatal root canal of the first molar were considered as reference, there was a 10.1% increase of the distance between maxillary bones (Fig. 2C-D). When the dental reference was the incisors, the mean distance between the occlusal third and middle third presented no significant changes (data not shown). Considering the area of midpalatal distraction, a significant RME was acquired (Fig. 3A-B) at both periods of 7 and 14 days.

3.2. RME led to an increased number of osteoblasts and had no significant impact in osteoclasts counting in the midpalatal suture

Since maxillae distraction was successful, we analyzed bone cells recruitment in midpalatal area. There were an increased number of osteoblasts under the three tensile forces at both time references (Fig. 4A-B). In contrast, no significant changes in osteoclasts numbers were observed comparing all groups (Fig. 4C-D). No inflammatory cells were observed in the suture area regardless the experimental time and tensile force (data not shown).

3.3. RME caused decrease of chondrocytes counting in the nasal area

Alike to the maxillary suture, the nasal cartilage also exhibited histopathological changes characterized by decreased number of chondrocytes in all experimental groups, with the exception for 0.28 N at 14 days (Fig. 4E-F). In addition, there was an increase of the intercellular matrix (ICM), chondrocyte clustering and hypertrophy in all groups and timepoints analyzed compared to respective controls. Changes were similar comparing force and time-point subgroups (Table 1).

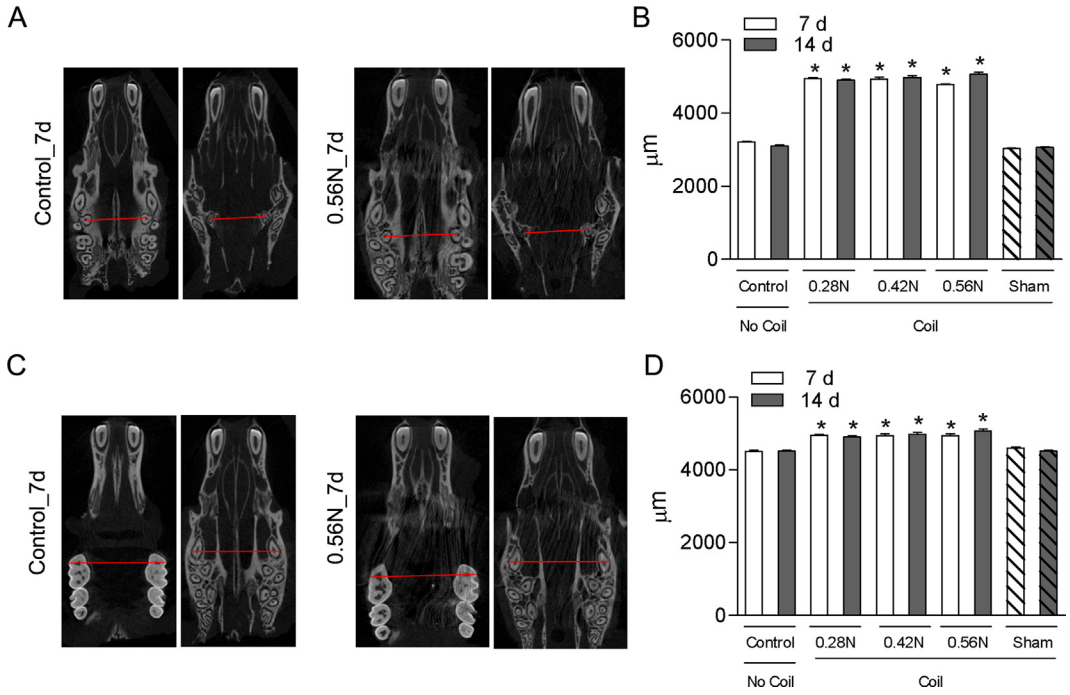

Fig. 2. Quantification of midpalatal suture distraction after RME. MicroCT images of control (without mechanical loading) (A, C) and 7 days after 0.56 N of force application (B, D). Measures in A and B were taken considering the occlusal third and middle third of the vestibular surface of the mesio-vestibular root of the first molar as reference. Measures of C and D considered the middle third and apical third of the palatal root canal of the first molar as reference. Six animals were used for control, 0.28 N, 0.42 N and 0.56 N groups and four mice for the sham operated groups at each timepoint. Data were expressed as mean ± standard deviation (SD). $P < 0.05$, * means different from Control group within the same timepoint.

3.4. RME up-regulates osteoblastic and osteoclastic markers

Next, we investigated the expression of bone resorption and apposition molecules after RME. Assessing osteoblasts markers, there were a greater expression of all analyzed markers at 7 and 14 days within the three tested forces (Fig. 5A-E). Almost all osteoblasts markers were increased at the second time point when compared with the first one, under all three applied forces. In exception, Runx2 and Alp presented no significant difference under 0.28 N of force at the first time point. The only marker that did not present significant change when comparing 7 days and 14 days was Col1a1 under 0.42 N of force (Fig. 5A-E).

Regarding osteoclasts, except the Rankl/Opg ratio at 14 days, all markers such as Rank, Ctsk, Timp1, Mmp9, MmpP13 at 7 and 14 days and Rankl/Opg at 7 days, were increased after RME when compared with mice not subjected to mechanical loading (control) (Fig. 6A-F). When the second time point (14 days) was compared with the first (7 days), we observed that RanklL/Opg, Ctsk, Timp1 showed decreased expression of these markers; Mmp9 and Rank (except under the force of 0.56 N for both markers and 0.28 N only for Mmp9, which had increased expression at 14 days) demonstrated similar results for both periods; and Mmp13 showed that all forces induced increase the expression at day 14.

Overall, while a significant expression of osteoclastic markers was seen early after force application, osteoblastic expression appears to be prominent at latter time point.

3.5. RME enhanced bone remodeling and associated molecular markers in the midpalatal suture

Except by BMD, sham operated and control mice had no difference in bone parameters in the midpalatal suture after RME (Fig. 7A-B). BMD was higher in the Sham in comparison to Control and all force magnitude groups. Lower BMD was exhibited in 0.28 N, 0.42 N and 0.56 N at day 7 compared to Control; and the density was reestablished at day 14 in 0.42 N and 0.56 N groups. BV/TV (0.42 N and 0.56 N groups) and BV (0.28 N, 0.42 N and 0.56 N groups) were diminished in comparison to Control and Sham (except for the 0.28 N BV/TV groups) mice at day 7, being the values increased in all forces magnitudes at the period of 14d when compared to 7d. No differences between groups were verified in the Tb.N in all experimental groups. Decreased Tb.Sp was determined in 0.28 N, 0.42 N and 0.56 N groups at day 7 in comparison to Sham mice; and diminished Tb.Th was exhibited in all forces groups compared to Control and Sham mice, being its number even lower in 0.56 N group compared to 0.28 N group and increased ad the period of 14d in comparison to 7d period (Fig. 7A-B). Threshold changes produced large differences in Tb.N, Tb.Sp, Tb.Th, BV and BV/TV, although the response profile remained similar in all tested thresholds (data not shown).

In addition, the expression of bone remodeling markers was analyzed. Except the expression of Tgfb3 with 0.28 N force at day 14 after RME, all magnitudes of forces have increased the expression of the bone markers in both timepoints. At day 7, increased levels of Tgfb1, Tgfb2, Bmp-2, Ctnnbl1, Wnt3a and Wnt5a were increase in groups 0.42 N and 0.56 N compared to group 0.28 N. The levels of Tgfb3 were augmented only in 0.42 N group compared to 0.28 N and Sost was increased only in 0.56 N animals compared to 0.28 N at period of 7 days. The expression of Tgfb3 and Bmp-2 was decreased in 0.56 N group compared to 0.42 N group, while Wnt3a was increased in 0.56 N group compared to 0.42 N at day 7. At day 14, RME augmented levels of Tgfb1, Tgfb2, Tgfb3, Sost, Wnt3 and Wnt3a in 0.42 N and 0.56 N force groups compared to 0.28 N. Ctnnbl1 levels were increased only in 0.56 N group compared to 0.28 N and Wnt5a was augmented only in 0.42 N group compared to 0.28 N force group at day 14. There was an increase of Tgfb3 and Wnt3 in 0.56 N group compared to 0.42 N group at day 14. Differences of bone markers expression

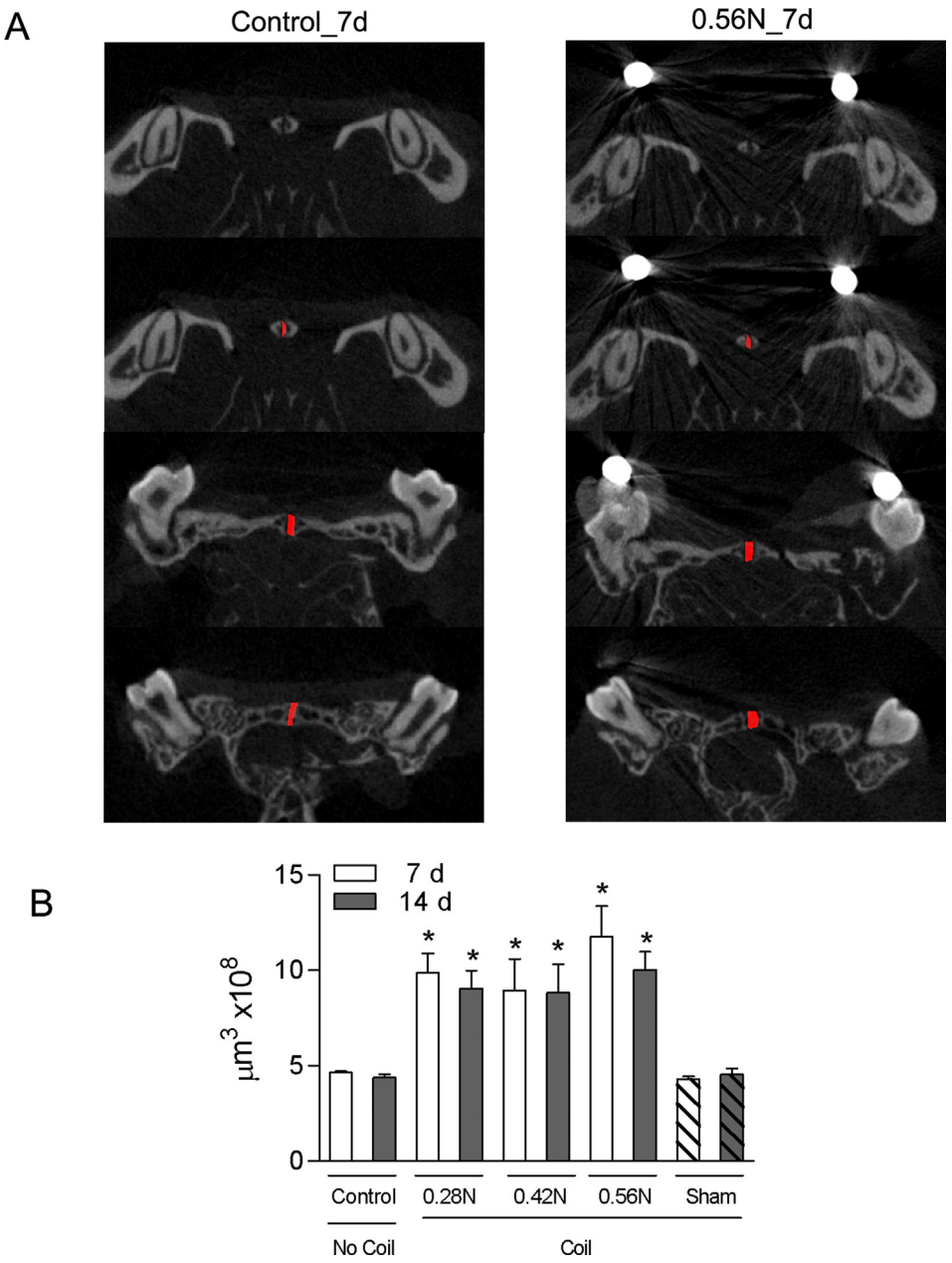

Fig. 3. Area gained in the midpalatal suture after RME. (A) MicroCT images of the antero-posterior palatal bone at the first molar level indicating the area of midpalatal distraction (red) in the Control and 0.56 N groups after 7 days of force application. (B) Amount of area obtained after RME in the midpalatal suture at different time point (7 and 14 days). Six animals were used for control, 0.28 N, 0.42 N and 0.56 N groups and four mice for the sham operated groups at each timepoint. Data were expressed as mean ± standard deviation (SD), $P < 0.05$, * means different from Control group within the same timepoint.

were verified between the timepoints of 7 and 14 days: Tgfb1 and Tgfb2 expression were decreased in 0.28 N, but increase at 0.42 N and 0.56 N groups; Tgfb3 levels were diminished in all magnitudes of force; Bmp-2 and Ctnnbl1 were reduced only in 0.42 N and 0.56 N groups; Sost and Wnt3a were increased in all experimental forces; Wnt3 expression was increased only in 0.56 N group; and no difference was seen in the expression of Wnt5a between both timepoints (Fig. 8A-I).

4. Discussion

We demonstrated that RME effectiveness is characterized by increase of the maxillary bones distance in the midpalatal suture, osteoblasts numbers and expression of key bone remodeling markers. Furthermore, the nasal cartilage was affected with reduction of chondrocytes. While different forces and timepoints resulted in a similar profile of suture opening, changes in molecular parameters and bone microstructure were time- and force-dependent.

RME has been employed as an experimental model to study bone remodeling (Cheng et al., 2018; Hou et al., 2007, 2009; Wu et al., 2017); however, there is a very restrict number, a total of four studies that were detailed in Table 2. Moreover, a variation of force application and the molecular findings associated with RME are little explored. Two studies using mice preconized the magnitude of force of 0.56 N (Hou et al., 2007, 2009). The magnitude of the force of the coil of our study was based on Hou et al. (Hou et al., 2007, 2009), however one more time-point force of 0.42 N was added in order to analyze if there was an incremental

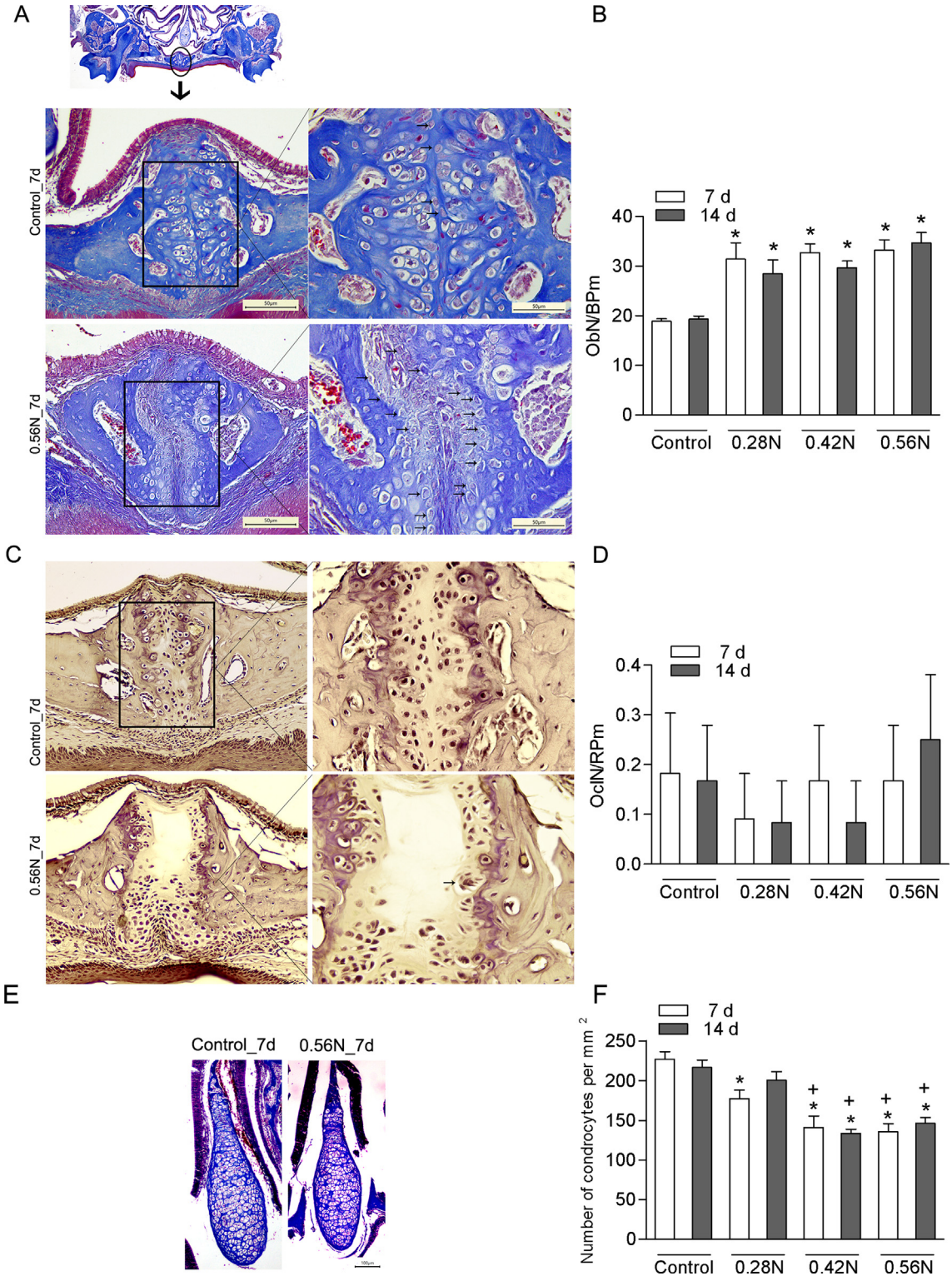

Fig. 4. Number of osteoblasts and osteoclasts at the midpalatal suture; and chondrocytes counting at the nasal area. (A) Representative images of osteoblasts in midpalatal suture after 7 days of RME (osteoblasts are indicated with black arrows). (B) Number of osteoblasts 7 and 14 days after RME. (C) Representative images of TRAP positive osteoclasts in the midpalatal suture after 7 days of RME (one osteoclast indicated with a black arrow). (D) Number of osteoclasts 7 and 14 days after RME. (E) Representative image of the Massońs staining of frontal sections of nasal cartilages of Control and 0.56 N groups after 7 days of RME. (F) Number of chondrocytes counted at the nasal cartilage. Six animals were used for each timepoint and experimental group. Data were expressed as mean ± standard deviation (SD). $P < 0.05$, * means different from Control group within the same timepoint; $^{+}$ means different from 0.28 N group within the same timepoint.

effect on the palatal suture and biomarkers expression along the period of 7 and 14 days. Regarding our findings, we observed that a lower magnitude of force such as 0.28 N and 0.42 N, during 7 days, promoted an efficient RME figuring that these forces are also within the physiological range for mice. Another relevant finding was that our RME protocol showed a similar impact using the upper first molars as reference, characterizing a homogeneous pattern of RME, as previously observed (Hou et al., 2007).

Table 1
Increase of the intercellular matrix (ICM), chondrocyte clustering and hypertrophy in all experimental groups of 7 and 14 days with all three forces of 0.28 N, 0.42 N and 0.56 N after RME.

	7d				14d			
	Control	0.28 N	0.42 N	0.56 N	Control	0.28 N	0.42 N	0.56 N
Increase of ICM	50%&*	83.33%*	83.33%*	100%*	33.3%*	83.33%*	100%*	100%*
Chondrocyte clustering	100%*	100%*	100%*	100%#	83.33%*	100%*	100%*	100%*
Hypertrophic chondrocytes	0%	50%*	33.3%*	50%*	0%	33.3%*	16.67%*	50%*

ICM: intercellular matrix. Data are expressed as the percentual of positive cases showing each histopathological change. *Score 1: change involves less than 50% of cartilage area. #Score 2: change involves more than 50% of cartilage area.

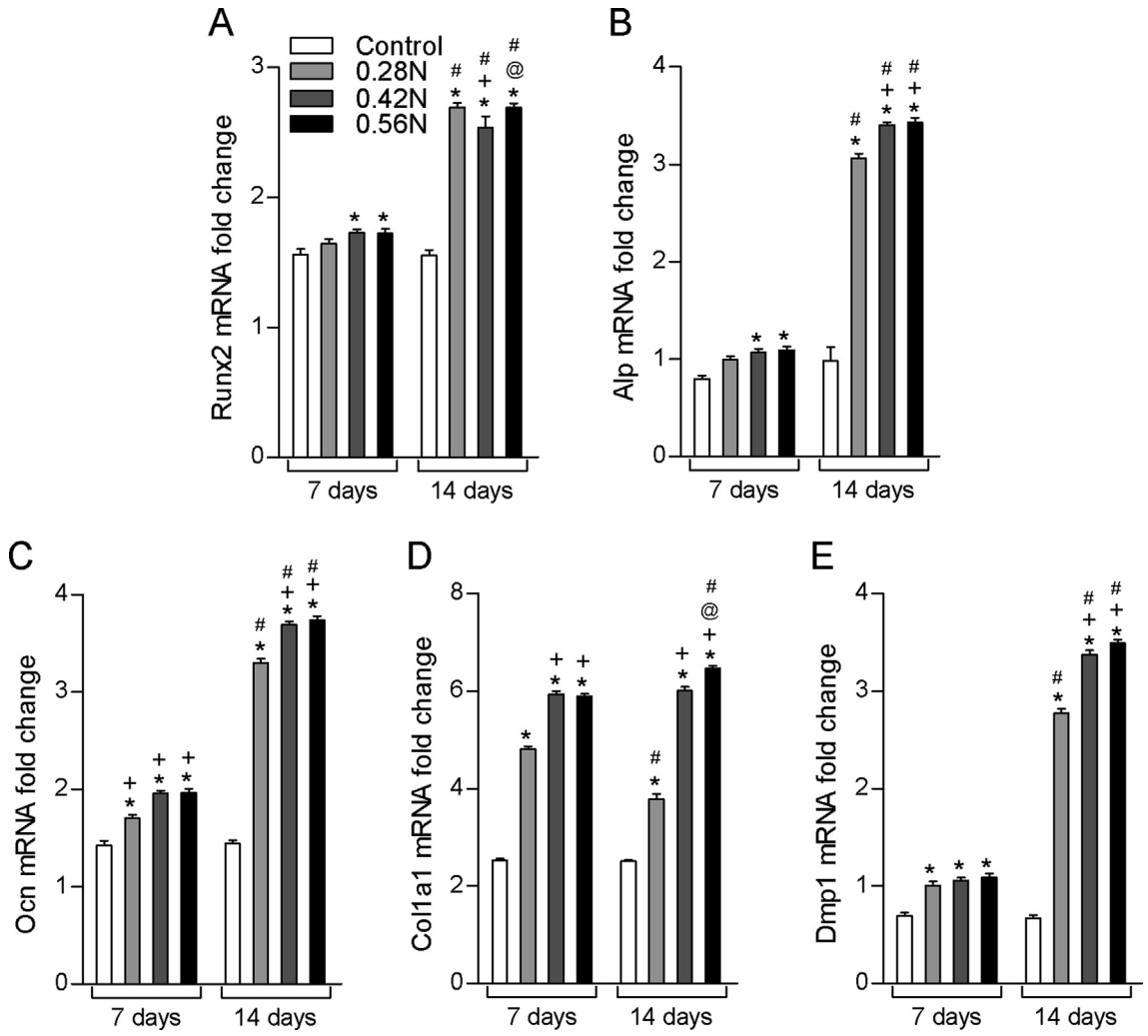

Fig. 5. Osteoblast markers expression in the midpalatal suture samples after 7 and 14 days of mechanical loading, under 0.28 N, 0.42 N or 0.56 N of force application. (A) Runt-related transcription factor 2 (Runx2); (B) Alkaline phosphatase (Alp); (C) Osteocalcin (Ocn); (D) Collagen type I Alpha 1 (Col1a1); and, (E) Dentin matrix acidic phosphoprotein 1 (Dmp1) $^{*}P < 0.05$ means different from the Control group at the same timepoint; $^{+}P < 0.05$ means different from 0.28 N at the same timepoint; $^{@}P < 0.05$ different from 0.42 N at the same timepoint; $^{\#}P < 0.05$ different from 7 days of mechanical loading under the same force magnitude. Six animals were used for each timepoint and experimental group. Data were expressed as mean ± standard deviation (SD).

Nevertheless, concerning the mean distance between incisors root, our findings are in disagreement with a recent study in rats (Wu et al., 2017) that observed an increased distance after RME. This divergence can be attributed to higher force magnitude and anatomical differences regarding animal type.

According to Hou et al. (2007) the magnitude of the force decays during the experimental period mainly due to expansion of the midpalatal suture and viscoelastic accommodation of the tissues, especially suture. In our study we did not measure the amount of magnitude reduction, however similar pattern of maxillary expansion was verified at both periods and alike to the maxillary suture, the nasal cartilage also exhibited histopathological changes suggesting force dissipation for neighboring structures. Despite the fact that important microCT and molecular parameters were only modified after 14 days, our results also should also be interpreted by considering that outcomes would be influenced by the decay of the force magnitude. Furthermore, the possible interference of force variation among animals and/or opening loops devices due the impossibility of force precision measurement in vivo should be considered as a limitation of study.

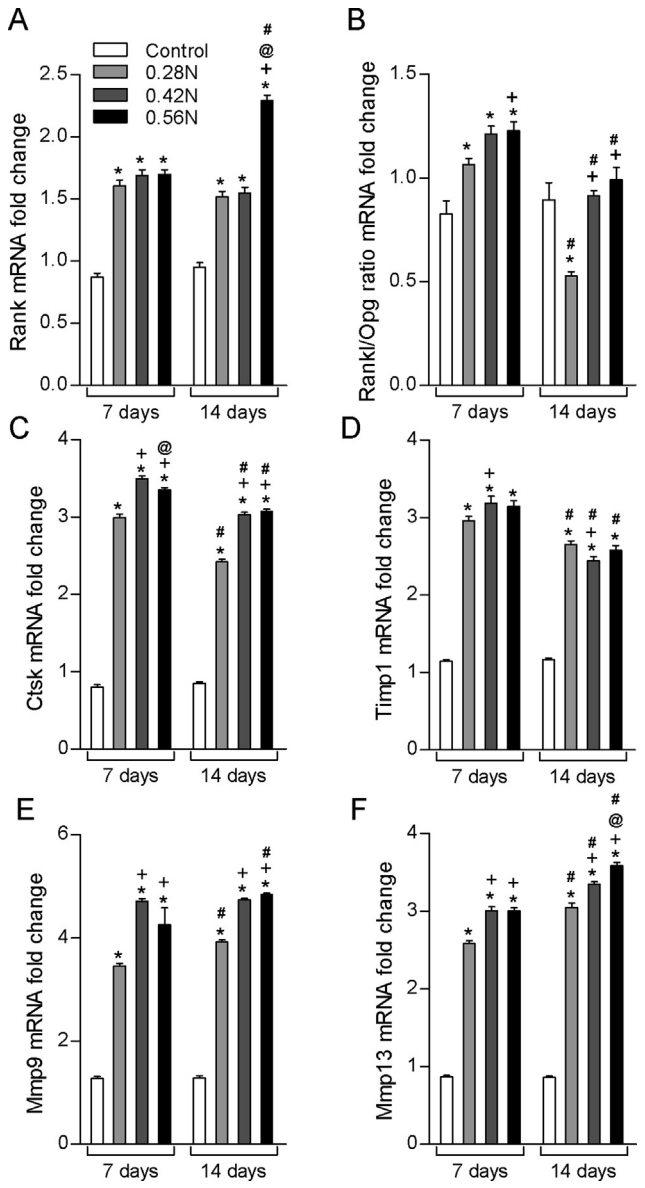

Fig. 6. Osteoclast markers expression in midpalatal samples after 7 and 14 days of mechanical loading, under 0.28 N, 0.42 N or 0.56 N of force application. (A) Receptor activator of nuclear factor kappa B (Rank); (B) Receptor activator of nuclear factor kappa B ligand (Rankl)/Osteoprotegerin (Opg) ratio; (C) Cathepsin K (Ctsk); (D) Tissue inhibitor of metalloproteinases-1 (Timp1); (E and F) Matrix metalloproteinases 9 and 13 (Mmp 9 and 13). $^{*}P < 0.05$ means different from the Control group at the same timepoint; $^{+}P < 0.05$ means different from 0.28 N at the same timepoint; $^{@}P < 0.05$ different from 0.42 N at the same timepoint; $^{\#}P < 0.05$ different from 7 days of mechanical loading under the same force magnitude. Six animals were used for each timepoint and experimental group. Data were expressed as mean ± standard deviation (SD).

The cellular and molecular events related to RME were reported in few studies. Regarding osteoblasts, we observed an increased number of these cells surrounding palatal bones, suggesting an active bone formation after 7 and 14 days of induced RME. It was suggested that RME increased expression of alkaline phosphatase and type I collagen mRNA-positive cells were identified in the periosteal cells close to palatal bones and distributed along the medial surface of newly formed bone and cartilage in the midpalatal suture (Hou et al., 2007). In agreement with our work, previous studied observed that the activity of osteoblast-like cells and the amount of new bone formation were stimulated after mechanical load (Cheng et al., 2018) and an increased layer of osteocalcin positive osteoblasts was covering the surface of the newly formed bone (Wu et al., 2017) subsequent to RME. Additionally, it was seen that RME would dissipate different mechanical stresses in the palatal bones, leading to an irregular distribution of osteoclasts and osteoblasts (Hou et al., 2007).

In accordance with Wu et al. (2017), no significant difference was seen in the osteoclast number after RME; however, Hou et al. (2007) suggested that the increased bone remodeling in the palatal suture after mechanical load was due to increase in the osteoclast count. One could speculate that these discrepant findings are due to the counting of TRAP-positive osteoclasts at different sites. For instance, while we counted the osteoclasts at the suture, Hou et al. (2007) analyzed them on the nasal side of the palatal bone surface.

Mechanical stress and inflammatory mediators may yield oxidative stress resulting in senescent and dedifferentiated chondrocytes with decreased survival (Ashraf et al., 2019). Accordingly, the nasal cartilage of mice exposed to RME presented decreased number of chondrocytes. In contrast, Hou et al. (Hou et al., 2009) did not find difference in chondrocytes after RME.

Osteoprogenitor cell proliferation, differentiation and activity is regulated by the expression of specific molecules (Aubin, 2001). For example, Runx2 has been shown to be an essential transcription factor for osteoblast differentiation; Dmp1 initiates osteoblast differentiation and regulates the expression of osteoblast-specific genes and orchestrates mineralized matrix formation; Col1a1 is early marker of osteoblast differentiation while Alp and Ocn are expressed by mature osteoblasts and used to quantify its activity (Huang et al., 2007). Consistently, RME induced increased expression of all the analyzed osteoblasts markers, suggesting an augment of osteoblastic differentiation and activity. Hou et al. (2009) did not observe difference in Runx2 levels after mechanical loading, but the analysis was performed at the nasal cartilage not in the palatal suture.

It is widely known that osteoclastogenesis is regulated by Rank/Rankl/Opg system (Aoki et al., 2010; Boyce and Xing, 2008). We verified an increased expression of Rank, Rankl and Opg at sites of sutures under mechanical force. Furthermore, the bone resorption is dependent on secretion of enzymes such as Timp-1, Catepk, Mmp9 and Mmp13 (Krishnan and Davidovitch, 2006; Wise and King, 2008) that were augmented after 7 and 14 days of RME. Accordingly, Mmp13, Rankl and Opg mRNA expression were increased after mechanical force in agreement with Hou et al. (2009) and Cheng et al. (2018). These factors have yet been found to play a definitive role in osteoclast development, although our results showed no difference in osteoclast numbers. Two possible explanations are: (1) RME acts via indirect resorption of bone (Hou et al., 2007; Melsen, 2001) being the osteoclasts localized on the nasal side of the palatal surface and not on the suture (Hou et al., 2007); and (2) there was not a compatibility on the time necessary to reach a target expression level after gene induction (Shamir et al., 2016). Internal signals such as the expression of the osteoclastic markers can induce the expression of one or several regulators, which in turn can trigger the appropriate cellular response, such as the osteoclast differentiation (Shamir et al., 2016).

There is an important limitation due to all covering RME in experimental model using rodents. RME in rodents leads to decrease of the original secondary cartilage and formation of new cartilage within the suture area on the oral side (Hou et al., 2007), characterizing an endochondral ossification. It differs from human intramembranous ossification observed after a RME (Melsen, 1972). It still an important model for the study of the mechanism of bone remodeling though; mainly when related to bone formation and analysis of the osteoblast response. Also, the presence of the coil creates artifacts that may confound measurements of bone

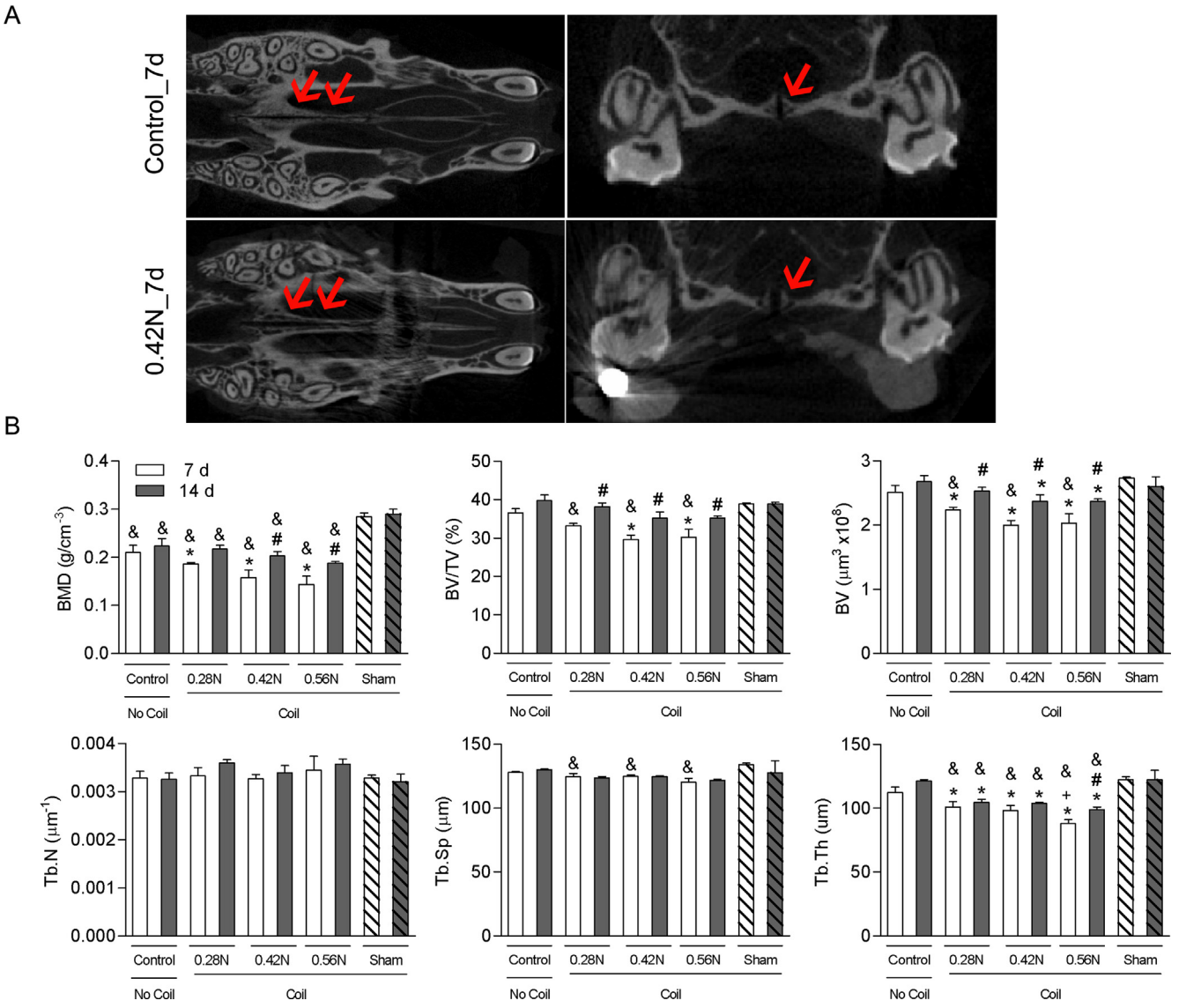

Fig. 7. (A) MicroCT images of the effects of RME on the microarchitecture of palatal bones, red arrown indicates the bone remodeling areas. (B) Bone mineral density (BMD g/cm^{-3}), percent bone volume/tissue volume (BV/TV %), bone volume (BV μm^3), trabecular number (Tb.N mm^{-1}), trabecular separation (Tb.Sp) and trabecular thickness (Tb.Th μm). $^{*}P < 0.05$ means different from the Control group at the same timepoint; $^{+}P < 0.05$ means different from 0.28 N at the same timepoint; $^{@}P < 0.05$ different from 0.42 N at the same timepoint; $^{\#}P < 0.05$ different from 7 days of mechanical loading under the same force magnitude; $^{\&}P < 0.05$ different from sham operated mice at the same timepoint. Six animals were used for control, 0.28 N, 0.42 N and 0.56 N groups and four mice for the sham operated groups at each timepoint. Data were expressed as mean ± standard deviation (SD).

density and makes difficult to determine a consistent threshold for all microCT parameters. In our study BMD was increased by the presence of the coil showing the need of two control groups (no coil and sham) and the decision of the threshold number was based on the image which was more similar to the raw one. RME has induced change in bone remodeling characterized by the decrease of BMD, BV/TV, BV and Tb.Th after 7 days of mechanical loading, while after 14 days of RME the midpalatal suture phenotype was restored. Mechanisms may rely on the expression of bone markers (Cheng et al., 2018; Hou et al., 2009). Tgfb can induce the transcription of different target genes that function in differentiation, chemotaxis, proliferation, and activation of many immune cells, leading to the activation of regulatory proteins. Roth et al. (1997) demonstrated that Tgfb1, Tgfb2 and Tgfb3 were present in human cranial sutures, being Tgfb2 the most expressed isoform and that Tgfb3 expression was increase at the margin of the normal patent sutures, suggesting a possible role of this isoform in the maintenance of cranial suture patency. Differently from Roth et al. (1997) Tgfb1 was the most expressed in the midpalatal suture of the mice and Tgfb3 has decreased expression along the analyzed period. Those differences might be explained because the study aforementioned was conducted in humans while our study was in mice.

Herein, we developed a standardized RME protocol in mice. In this model, force magnitudes of 0.28 N, 0.42 N and 0.56 N at 7 and 14 days resulted in a similar profile of suture opening but changes in bone microstructure and expression of target genes were time- and force-dependent. Therefore, these parameters characterize bone cells recruitment and activity in the suture after mechanical load, proving the reliability of this protocol as a model for bone remodeling.

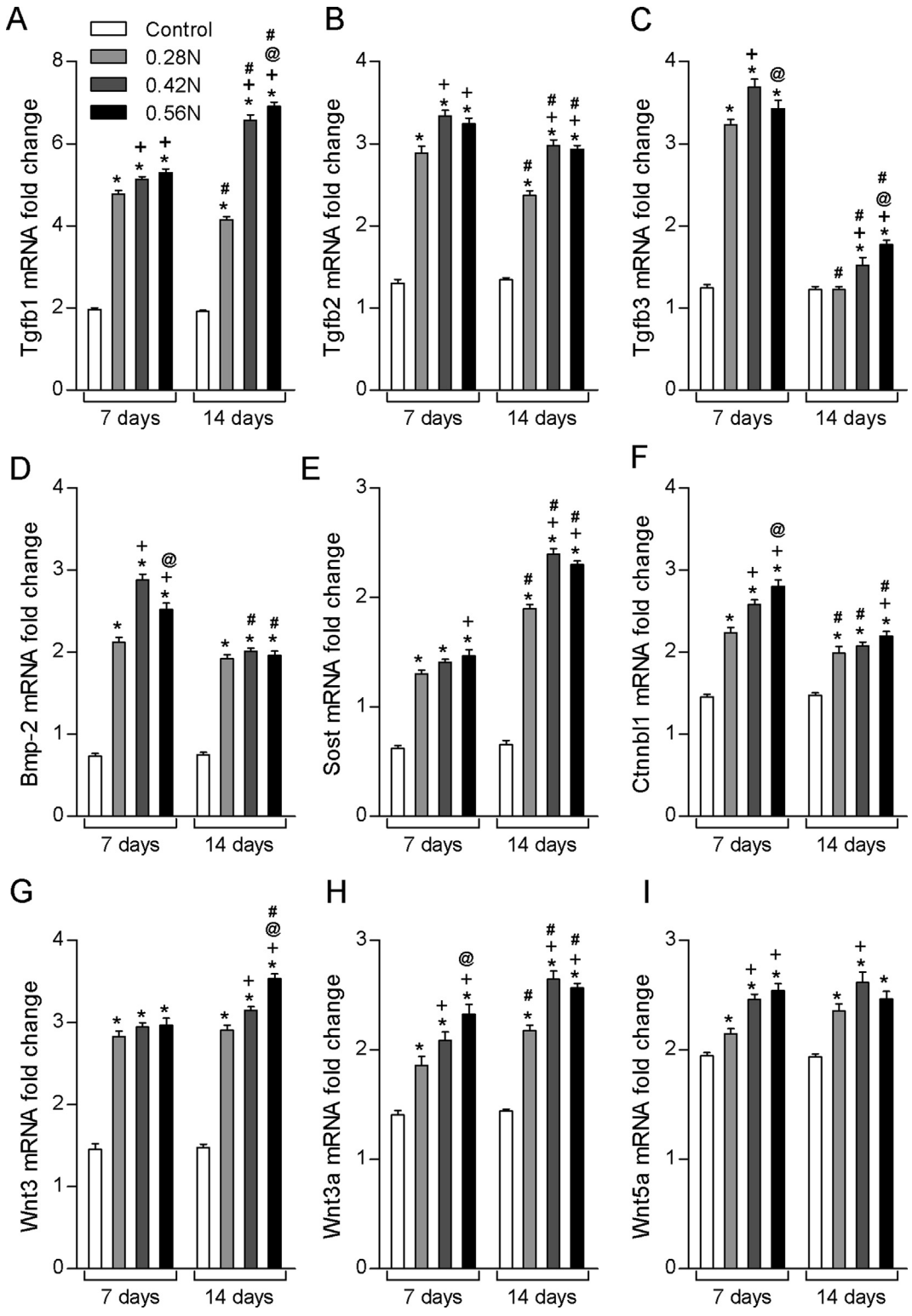

Fig. 8. Bone remodeling markers expression in midpalatal samples after 7 and 14 days of mechanical loading, under 0.28 N, 0.42 N or 0.56 N of force application. (A, B and C) Transforming growth fator beta 1, 2 and 3 (Tgfb 1; Tgfb 2 and Tgfb3) respectively; (D) Bone morphogenetic protein 2 (Bmp-2); (E) Sclerostin (Sost); (F) Beta-catenin-like protein 1 (Ctnnbl); and, (G, H and I) Wnt signaling pathways 3, 3a and 5a (Wnt 3, Wnt 3a and Wnt 5a) respectively. $^{*}P < 0.05$ means different from the Control group at the same timepoint; $^{+}P < 0.05$ means different from 0.28 N at the same timepoint; $^{@}P < 0.05$ different from 0.42 N at the same timepoint; $^{\#}P < 0.05$ different from 7 days of mechanical loading under the same force magnitude. Six animals were used for each timepoint and experimental group. Data were expressed as mean ± standard deviation (SD).

Table 2
Studies using RME as experimental model.

Authors/Year	Aim(s)	Time points (days)	Force magnitude	Force calibration	Animals	Appliance	Analysis	Main results
Hou et al. (2007)	Describe how an expansive force across the midpalatal suture induces a suture remodeling and new bone formation	1, 3, 5, 7, 14 and 28	0.56 N	Initial force = 0.56 N. At day 7 = 0.28 N At day 14 = 0.05 N	Mice	Opening loops using 0.014-inch stainless steel orthodontic wire	MicroCT; FC; histology and HC; IHC; ISH	RME results in 1) expansion and reorientation of collagen fibers; 2) decrease of suture cartilage and augment of osteoclasts Periosteal cells are the major source of new bone and cartilage formation
Hou et al. (2009)	Elucidate the function of PC1 in different cell types and at different differentiation stages	1, 3, 7 and 14	0.56 N	Initial force = 0.56 N At day 7 = 0.28 N and at day 14 = 0.05 N	Mice	Opening loops using 0.014-inch stainless steel orthodontic wire	FC; Histology, IHC, ISH and TUNEL; β-galactosidase staining and qPCR	Wnt1Cre; Pkd1 mice under RME presented: 1) less new bone formation; 2) low expression of Col2a1; 3) increased periosteal cell apoptosis and chondrocyte apoptosis in nasal cartilage; 4) accelerated ossification of nasal cartilage upon midpalatal suture expansion; 5) altered expression of regulators of chondrocyte differentiation, matrix degradation and vascular invasion
Wu et al. (2017)	Characterize the special finger-like pattern of bone formation in suture guided by tensile stimuli	1, 3, 5 and 7	1.76 N (linear regression)	The force/deformation was calibrated using 3 springs activated at four force levels. The force was measured using a force gauge, and the amount of deflection was determined using a ruler	Rat	Opening loops using 0.014-inch stainless steel orthodontic wire	MicroCT; FC; histology and HC; IHC	The inter-incisor width of expanded rats increased quickly at the first day; and at later time points, the rate of increase was reduced and remained nearly constant Larger volume of new bone was formed on the nasal side than on the oral side of sutures The direction of deflection matched the direction of the stretch force
Cheng et al. (2018)	To investigate the effect of lactoferrin on bone resorption on the midpalatal sutures during RME	1, 4, 7, and 14	50 ± 5 g	The appliances were activated immediately after bonding	Rat	An expansion spring with 2 helices was fabricated with 0.014-in orthodontic wire	MicroCT; histology and HC; IHC and qPCR	Bone volume/tissue volume ratio and the relative bone mineral density of the suture bone were significantly increased in animals treated with lactoferrin Lactoferin stimulated the activity of osteoblast-like cells and the amount of new bone formation after RME while there were no difference in the osteoclasts RANKL and OPG were inclrease after RME but no difference were seen between the expansion control and expasion lactoferrin groups
Present study	To analyze the kinetics of molecular bone markers and bone cells recruitment by using a standardized RME protocol	7 or 14	0.28 N, 0.42 N 0.56 N	Tension gauge	Mice	Opening loops using 0.014-inch stainless steel orthodontic wire	MicroCT; histology; qPCR	RME and increased number of osteoblasts, but not osteoclasts count; decreased number of chondrocytes RME yielded significant increase expression of osteoblastic markers such as Ocn, Dmp1, RunX2, Col1a1, Alp; also increased osteoclastic markers as Rank, Rankl, Opg, Ctsk, Mmp9 and Mmp13; and enhanced bone remodeling markers such as Tgfb 1, Tgfb 2 and Tgfb3, Bmp-2, Sost, Ctnnbl, Wnt 3, Wnt 3a and Wnt 5a Increase in bone remodeling in the midpalatal suture evaluated by decreased BMD, BV/TV, BV and Tb.Th The ideal amount of force and timing required to promote optimal RME is 0.42 N for 7 days

N, Newton; g, grams; MicroCT, Microcomputed tomography; FC, Fluorescence labeling; HC, Histochemistry; IHC, Immunohistochemistry; ISH, In situ hybridization; RME, Midpalatal suture expansion; PC1, Polycystin-1; TUNEL, Terminal deoxynucleotidyl-transferaseemediated dUTP- FITC nick-end labeling; qPCR, Real-time quantitative Polymerase Chain Reaction; Pkd1, Polycystic kidney disease 1; Col2a1, Collagen, type II, a1; Rankl,receptor activator of nuclear factor kappa B ligand; Opg,osteoprotegerin; Osteocalcin (Ocn); Dentin matrix acidic phosphoprotein 1 (Dmp1); Runt-related transcription factor 2 (Runx2); Collagen type I alpha 1 (Col1a1); Alkaline phosphatase (Alp); Receptor activator of nuclear factor kappa B (Rank); Cathepsin K (Ctsk); Matrix metalloproteinases 9 and 13 (Mmp9 and 13); Transforming growth fator beta 1, 2 and 3 (Tgfb 1; Tgfb 2 and Tgfb3), Bone morphogenetic protein 2 (Bmp-2), Sclerostin (Sost), Beta-catenin-like protein 1 (Ctnnbl) and Wnt signaling pathways 3, 3a and 5a (Wnt 3, Wnt 3a and Wnt 5a); bone volume/tissue volume (BV/TV %), bone volume (BV μm3) and trabecular thickness (Tb.Th μm).

5. Financial support

This work was supported by Fundação de Amparo à Pesquisa do Estado de Minas Gerais (FAPEMIG), Conselho Nacional de Desenvolvimento Científico e Tecnológico (CNPq), Coordenação de Aperfeiçoamento de Pessoal de Nível Superior (CAPES), Pró-reitoria de Pesquisa – Universidade Federal de Minas Gerais, Departamento Administrativo de Ciencia, Tecnología e Innovación (COLCIENCIAS).

Declaration of Competing Interest

The authors declare that they have no known competing financial interests or personal relationships that could have appeared to influence the work reported in this paper.

Appendix A. Supplementary material

Supplementary data to this article can be found online at https://doi.org/10.1016/j.jbiomech.2020.109880.

References

Aoki, S., Honma, M., Kariya, Y., Nakamichi, Y., Ninomiya, T., Takahashi, N., Udagawa, N., Suzuki, H., 2010. Function of OPG as a traffic regulator for RANKL is crucial for controlled osteoclastogenesis. J. Bone Mineral Res.: Off. J. Am. Soc. Bone Mineral Res. 25, 1907–1921.

Ashraf, S., Kim, B.J., Park, S., Park, H., Lee, S.H., 2019. RHEB gene therapy maintains the chondrogenic characteristics and protects cartilage tissue from degenerative damage during experimental murine osteoarthritis. Osteoarthritis Cartilage 27, 1508–1517.

Aubin, J.E., 2001. Regulation of osteoblast formation and function. Rev. Endocr. Metab Disord. 2, 81–94.

Bishara, S.E., Staley, R.N., 1987. Maxillary expansion: clinical implications. Am. J. Orthod. Dentofac. Orthop. Off. Publ. Am. Assoc. Orthodontists Constit. Soc. Am. Board Orthodontics 91, 3–14.

Bouxsein, M.L., Boyd, S.K., Christiansen, B.A., Guldberg, R.E., Jepsen, K.J., Muller, R., 2010. Guidelines for assessment of bone microstructure in rodents using micro-computed tomography. J. Bone Mineral Res. Off. J. Am. Soc. Bone Mineral Res. 25, 1468–1486.

Boyce, B.F., Xing, L., 2008. Bruton and Tec: new links in osteoimmunology. Cell Metab. 7, 283–285.

Byron, C.D., Borke, J., Yu, J., Pashley, D., Wingard, C.J., Hamrick, M., 2004. Effects of increased muscle mass on mouse sagittal suture morphology and mechanics. Anat. Rec. A Discov. Mol. Cell Evol. Biol. 279, 676–684.

Cheng, Y., Sun, J., Zhou, Z., Pan, J., Zou, S., Chen, J., 2018. Effects of lactoferrin on bone resorption of midpalatal suture during rapid expansion in rats. Am. J. Orthodontics Dentofacial Orthopedics: Off. Publ. Am. Assoc. Orthodontists Constit. Soc. Am. Board Orthodontics 154, 115–127.

Copray, J.C., Jansen, H.W., Duterloo, H.S., 1985. Effects of compressive forces on proliferation and matrix synthesis in mandibular condylar cartilage of the rat in vitro. Arch. Oral Biol. 30, 299–304.

da Silva Filho, O.G., Magro, A.C., Capelozza Filho, L., 1998. Early treatment of the Class III malocclusion with rapid maxillary expansion and maxillary protraction. Am. J. Orthodontics Dentofacial Orthopedics: Off. Publ. Am. Assoc. Orthodontists Constit. Soc. Am. Board Orthodontics 113, 196–203.

Guest, S.S., McNamara Jr., J.A., Baccetti, T., Franchi, L., 2010. Improving Class II malocclusion as a side-effect of rapid maxillary expansion: a prospective clinical study. Am. J. Orthodontics Dentofacial Orthopedics: Off. Publ. Am. Assoc. Orthodontists Constit. Soc. Am. Board Orthodontics 138, 582–591.

Hadjidakis, D.J., Androulakis, I.I., 2006. Bone remodeling. Ann N Y Acad Sci 1092, 385–396.

Henderson, J.H., Chang, L.Y., Song, H.M., Longaker, M.T., Carter, D.R., 2005. Age-dependent properties and quasi-static strain in the rat sagittal suture. J. Biomech. 38, 2294–2301.

Hinton, R.J., 1988. Response of the intermaxillary suture cartilage to alterations in masticatory function. Anatomical Rec. 220, 376–387.

Hou, B., Fukai, N., Olsen, B.R., 2007. Mechanical force-induced midpalatal suture remodeling in mice. Bone 40, 1483–1493.

Hou, B., Kolpakova-Hart, E., Fukai, N., Wu, K., Olsen, B.R., 2009. The polycystic kidney disease 1 (Pkd1) gene is required for the responses of osteochondroprogenitor cells to midpalatal suture expansion in mice. Bone 44, 1121–1133.

Huang, W., Yang, S., Shao, J., Li, Y.P., 2007. Signaling and transcriptional regulation in osteoblast commitment and differentiation. Front. Biosci. 12, 3068–3092.

Jiao, H., Xiao, E., Graves, D.T., 2015. Diabetes and its effect on bone and fracture healing. Curr. Osteoporos Rep. 13, 327–335.

Kantomaa, T., Tuominen, M., Pirttiniemi, P., 1994. Effect of mechanical forces on chondrocyte maturation and differentiation in the mandibular condyle of the rat. J. Dent. Res. 73, 1150–1156.

Krishnan, V., Davidovitch, Z., 2006. Cellular, molecular, and tissue-level reactions to orthodontic force. Am. J. Orthodontics Dentofacial Orthopedics: Off. Publ. Am. Assoc. Orthodontists Constit. Soc. Am. Board Orthodontics 129 (469), e461–432.

Lima, I.L.A., Silva, J.M.D., Rodrigues, L.F.D., Madureira, D.F., Fonseca, A.C., Garlet, G.P., Teixeira, M.M., Russo, R.C., Fukada, S.Y., Silva, T.A.D., 2017. Contribution of atypical chemokine receptor 2/ackr2 in bone remodeling. Bone 101, 113–122.

Macari, S., Madeira, M.F.M., Lima, I.L.A., Pereira, T.S.F., Dias, G.J., Cirelli, J.A., de Molon, R.S., Fukada, S.Y., Szawka, R.E., Garlet, G.P., Teixeira, M.M., Silva, T.A., 2018a. ST2 regulates bone loss in a site-dependent and estrogen-dependent manner. J. Cell. Biochem.

Macari, S., Sharma, L.A., Wyatt, A., da Silva, J.M., Dias, G.J., Silva, T.A., Szawka, R.E., Grattan, D.R., 2018b. Lactation induces increases in the RANK/RANKL/OPG system in maxillary bone. Bone 110, 160–169.

McNamara Jr., J.A., 2006. Long-term adaptations to changes in the transverse dimension in children and adolescents: an overview. Am. J. Orthodontics Dentofacial Orthopedics: Off. Publ. Am. Assoc. Orthodontists Constit. Soc. Am. Board Orthodontics 129, S71–74.

Melsen, B., 1972. A histological study of the influence of sutural morphology and skeletal maturation on rapid palatal expansion in children. Trans. Eur. Orthod. Soc., 499–507

Melsen, B., 2001. Tissue reaction to orthodontic tooth movement–a new paradigm. Eur. J. Orthod. 23, 671–681.

Raggatt, L.J., Partridge, N.C., 2010. Cellular and molecular mechanisms of bone remodeling. J. Biol. Chem. 285, 25103–25108.

Raisz, L.G., 1999. Physiology and pathophysiology of bone remodeling. Clin. Chem. 45, 1353–1358.

Ren, Y., Hazemeijer, H., de Haan, B., Qu, N., de Vos, P., 2007. Cytokine profiles in crevicular fluid during orthodontic tooth movement of short and long durations. J. Periodontol. 78, 453–458.

Riancho, J.A., Delgado-Calle, J., 2011. Osteoblast-osteoclast interaction mechanisms. Reumatol. Clin. 7 (Suppl 2), S1–S4.

Roth, D.A., Gold, L.I., Han, V.K., McCarthy, J.G., Sung, J.J., Wisoff, J.H., Longaker, M.T., 1997. Immunolocalization of transforming growth factor beta 1, beta 2, and beta 3 and insulin-like growth factor I in premature cranial suture fusion. Plast. Reconstr. Surg. 99, 300–309. discussion 310–306.

Schett, G., Teitelbaum, S.L., 2009. Osteoclasts and arthritis. J. Bone Mineral Res.: Off. J. Am. Soc. Bone Mineral Res. 24, 1142–1146.

Shamir, M., Bar-On, Y., Phillips, R., Milo, R., 2016. SnapShot: timescales in cell biology. Cell 164, (1302–1302) e1301.

Taddei, S.R., Moura, A.P., Andrade Jr., I., Garlet, G.P., Garlet, T.P., Teixeira, M.M., da Silva, T.A., 2012. Experimental model of tooth movement in mice: a standardized protocol for studying bone remodeling under compression and tensile strains. J. Biomech. 45, 2729–2735.

Tanaka, Y., Nakayamada, S., Okada, Y., 2005. Osteoblasts and osteoclasts in bone remodeling and inflammation. Curr. Drug Targets Inflamm. Allergy 4, 325–328.

Vij, K., Mao, J.J., 2006. Geometry and cell density of rat craniofacial sutures during early postnatal development and upon in vivo cyclic loading. Bone 38, 722–730.

Wise, G.E., King, G.J., 2008. Mechanisms of tooth eruption and orthodontic tooth movement. J. Dent. Res. 87, 414–434.

Wu, B.H., Kou, X.X., Zhang, C., Zhang, Y.M., Cui, Z., Wang, X.D., Liu, Y., Liu, D.W., Zhou, Y.H., 2017. Stretch force guides finger-like pattern of bone formation in suture. PLoS ONE 12, e0177159.